Charge state distribution and its equilibration of 2 MeV/u sulfur ions passing through carbon foils

M. Imai [a,*], M. Sataka [b], K. Kawatsura [c], K. Takahiro [c],
K. Komaki [d], H. Shibata [a], H. Sugai [b], K. Nishio [b]

[a] *Department of Nuclear Engineering, Kyoto University, Sakyo, Kyoto 606-8501, Japan*
[b] *Department of Materials Science, Japan Atomic Energy Research Institute, Tokai, Ibaraki 319-1195, Japan*
[c] *Department of Chemistry and Materials Technology, Kyoto Institute of Technology, Sakyo, Kyoto 606-8585, Japan*
[d] *Institute of Physics, Graduate School of Arts and Sciences, University of Tokyo, Meguro, Tokyo 153-8902, Japan*

Available online 12 January 2005

Abstract

Charge state distributions of 2.0 MeV/u sulfur ions of various initial charge states (6, 10, 11, 13+) after passing through 0.9, 1.5, 2.0, 3.0, 4.7, 6.9 and 10 μg/cm^2 carbon foils have been studied. It is observed that the processes involving the L-shell electrons are equilibrated within the target thickness of ∼5 μg/cm^2 and the charge equilibration over this thickness is ruled by the K-shell processes. Measured charge state distributions do not flat off to establish equilibrium within the measured thicknesses, but the mean charge states almost saturate to 12.4 for all initial charge states examined. Calculation with ETACHA code, developed by Rozet et al. [Nucl. Instr. and Meth. B 107 (1996) 67], is employed, although the present impact energy is lower than the assumed region for the code.
© 2004 Elsevier B.V. All rights reserved.

1. Introduction

Charge state evolution is one of the most important aspects in ion–solid interactions. Various processes [1], such as electron capture, ionization, excitation, vacancy production [2] and the consequent phenomena like energy loss and stopping [3], are closely related with the projectile charge state evolution in the target. Equilibrium charge state distributions for various collision systems have been extensively investigated and compiled [4–7], although the charge state distribution somewhat changes upon exiting the target foil [1,8]. It is also important in rather technical field

---
[*] Corresponding author. Tel./fax: +81 75 753 5846.
E-mail address: imai@nucleng.kyoto-u.ac.jp (M. Imai).

of design and operation of accelerators, spectrometers and so on [9].

Charge state distributions before its equilibrium have also been studied experimentally as well as theoretically by solving rate equations. On the earlier stage, only the charge exchange cross sections were included in the equations, but the continuous efforts have made it obvious for solid targets that excited states play important roles in the electron loss [8,10] and that the production and transport of inner shell vacancies of the projectiles have to be studied [11]. Following the developments of large accelerator facilities, projectiles at up to 1000 MeV/u have come to be under the investigations, increasing the importance of pre-equilibrium charge state information [7,12]. For the medium energy region over 10 MeV/u, Rozet et al. developed a PC based code ETACHA [13,14], calculating charge state distributions of ions with at most 28 electrons.

As for the S^{q+} + C collision system, Clark et al. have measured the equilibrium charge state distributions at 1.04 and 4.12 MeV/u [15] and Scharfer et al. have measured the charge state distributions of 69.5–141.8 MeV $S^{(6-10)+}$ prior to and after the equilibrium [16]. Gray et al. showed the experimental results for 54 MeV $S^{11,15+}$ projectiles with their calculations based on a new model including the production and transport of K-shell vacancies [11]. Shima et al. reported the equilibrium charge state distribution at 2.0 MeV/u [17], and Betz et al. presented the results for 125 MeV $S^{16,15+}$ ions with their calculations including the presence of lower charge state fractions down to 7 electron system [18].

The authors also have been devoted to studying collision phenomena inside the solid target using 2.0 or 2.5 MeV/u sulfur ions passing through thin carbon foils [19–21], and, in the present, performed another new experiment to derive the charge state distributions of 2.0 MeV/u S^{q+} (q = 6, 10, 11, 13) ions after penetration of thin carbon foils of 0.9– 10 μg/cm^2, which cover the non-equilibrium region.

2. Experiments

The present experiments were performed at the tandem accelerator facility at the Japan Atomic

Energy Research Institute (JAERI), Tokai. A beam of 2.0 MeV/u (64 MeV) S^{6+} ion was provided from the tandem accelerator. A post-stripper C-foil of ~20 μg/cm^2 in thickness was placed after the energy analyzing magnet to produce higher charge state fractions. The energy losses at the post-stripper foil were assumed to be at most 0.7% by our separate measurement of cusp electron energies with zero-degree electron spectroscopy [19,21]. The primary S^{6+} or post-stripped S^{q+} (q = 10, 11, 13) ion beam was directed by a switching magnet to self-support carbon target foils of 0.9, 1.5, 2.0, 3.0, 4.7, 6.9 and 10 μg/cm^2 in thickness. The charge state distributions after foil penetration were measured using the heavy ion magnetic spectrometer ENMA [22] and position-sensitive gas chamber detector. The vacuum condition inside the spectrometer was maintained below 10^{-6} Pa and was good enough to eliminate the background charge exchange collisions with residual gas, which was confirmed by measurements without target foil.

3. Results and discussion

Charge state fractions for 2.0 MeV/u S^{6+}, S^{10+}, S^{11+} and S^{13+} ions incident after passing through the carbon foil targets of 0.9, 1.5, 2.0, 3.0, 4.7, 6.9 and 10 μg/cm^2 are shown in Fig. 1, and the numerical values for S^{6+} are tabulated in Table 1, with those for 69.5 MeV S^{6+} through 12 μg/cm^2 target by Scharfer et al. [16] and for 63.8 MeV S ion after the equilibrium by Shima et al. [17] Typical errors for the charge fractions are estimated to be 20% for the smallest fractions around 1.0×10^{-5} and less than 0.5% for the largest fractions around 0.3. Also tabulated are mean charge $\bar{q} = \sum_q q F(q)$ and charge distribution width $d = [\sum_q (q - \bar{q})^2 F(q)]^{1/2}$, where q and $F(q)$ are charge state and its fraction, respectively. In Fig. 2, the mean charge states and the distribution widths for all the incident ions are plotted with the results obtained with ETACHA code (see below). Comparing the charge state distributions in Fig. 1, it can be seen that the cases of S^{10+}, S^{11+} and S^{13+} incident ions give almost the same distribution, regardless of the initial charge state, when
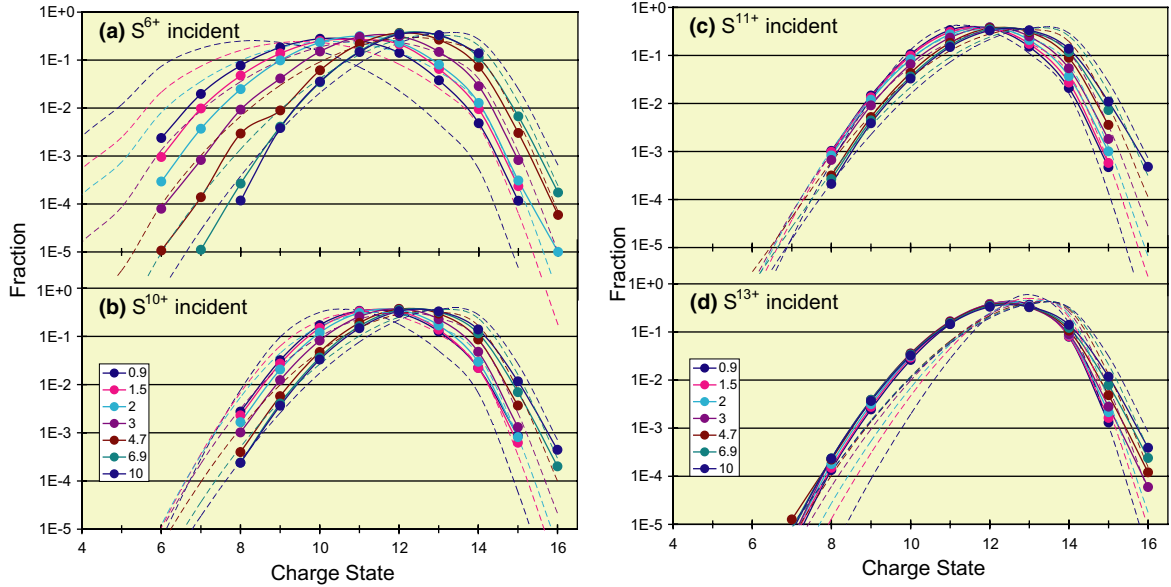
Fig. 1. Charge state distributions of 2.0 MeV/u (a) S^{6+}, (b) S^{10+}, (c) S^{11+} and (d) S^{13+} ions incident through carbon foil targets of 0.9, 1.5, 2.0, 3.0, 4.7, 6.9 and 10 μg/cm^2 in thickness (filled circles). The full lines are for eyeguiding only. The dashed lines are calculated fractions with the ETACHA code.

Table 1
Charge state fractions, mean charge states and charge distribution widths of 2.0 MeV/u S^{6+} ion incident after passing through carbon foil targets

Foil thickness (μg/cm²)	Charge state fraction											Mean charge	Width
	S^{6+}	S^{7+}	S^{8+}	S^{9+}	S^{10+}	S^{11+}	S^{12+}	S^{13+}	S^{14+}	S^{15+}	S^{16+}		
0.9	2.37−3	0.0196	0.0769	0.184	0.278	0.255	0.141	0.0377	4.80−3	1.16−4	–	10.3	1.37
1.5	9.50−4	9.78−3	0.0477	0.137	0.249	0.267	0.213	0.0653	9.45−3	2.35−4	–	10.7	1.36
2.0	2.94−4	3.69−3	0.0248	0.0985	0.233	0.315	0.231	0.0804	0.0127	3.08−4	1.00−5	10.9	1.26
3.0	7.92−5	8.26−4	9.28−3	0.0414	0.151	0.305	0.315	0.148	0.0285	8.21−4	–	11.4	1.18
4.7	1.07−5	1.39−4	2.93−3	8.91−3	0.0615	0.217	0.367	0.267	0.0722	3.01−3	5.92−5	12.0	1.08
6.9	–	1.11−5	2.65−4	4.08−3	0.0344	0.153	0.363	0.325	0.113	6.70−3	1.73−4	12.3	1.03
10	–	–	1.18−4	3.83−3	0.0355	0.147	0.343	0.331	0.139	–	–	12.4	1.03
12[a]	–	–	–	–	0.04	0.173	0.367	0.304	0.110	0.006	–	12.3	1.02
Equilibrium[a]	–	–	2−4	2.9−3	0.0263	0.122	0.292	0.338	0.195	0.0226	1.0−3	12.62	1.10

Typical errors are estimated to be 20% for the smallest fractions and less than 0.5% for the largest fractions. Expression like 2.37−3 denotes 2.37×10^{-3}.

[a] Data for 12 μg/cm^2 target are for 69.5 MeV S^{6+} taken from Scharfer et al. [16] and data for the equilibrium are taken from the experiment by Shima et al. [17] for 63.8 MeV.

the target thickness grows larger than 4.7 μg/cm^2 and that for S^{6+} incident ion also merges as the target thickness exceeds 6.9 μg/cm^2. When the target thickness grows from 4.7 to 10 μg/cm^2, the common distribution shifts up a bit for the higher charge states of (14–16)+, while it stays unchanged

for the lower charge states of (8–13)+. This behavior can also be found in Fig. 2 that the mean charge states and the distribution widths for S^{10+}, S^{11+} and S^{13+} ion incidences show common slight increase in the target thickness region larger than 4.7 μg/cm^2. This tendency implies that the
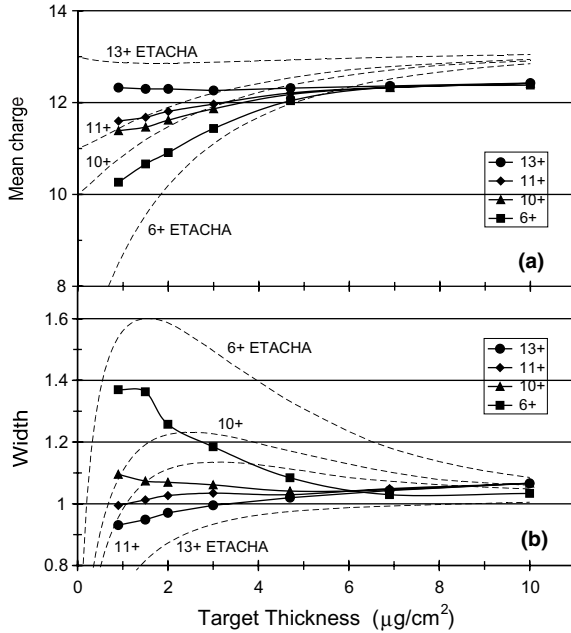
Fig. 2. (a) Mean charge states and (b) distribution widths for 2.0 MeV/u S^{6+}, S^{10+}, S^{11+} and S^{13+} ions incident after passing through carbon foil targets (filled symbols). The full lines are for eyeguiding only. The dashed lines are calculated values with the ETACHA code.

processes involving the L-shell electrons are equilibrated within the target thickness of $\sim 5\,\mu g/cm^2$ and the charge equilibration over this thickness is ruled by the K-shell processes, namely the K-shell electron loss and excitation.

The charge fractions do not flat off in the measured foil thickness range, but from the viewpoint of the mean charge, it almost reaches its equilibrium value of 12.4 as illustrated in Fig. 2(a). This trend is consistent with the minimum thickness of solid target required to establish charge state equilibrium, derived to be $10.4\,\mu g/cm^2$ with an expression by Besenbacher et al. [23],

$$N\Delta R[\text{atoms/cm}^2] \geqslant 2 \times 10^{20} \frac{1}{Z_2} \left(\frac{E[\text{MeV}]}{Z_1 A_1[\text{amu}]} \right)^2,$$

where N and ΔR denote target atomic density and thickness, Z_1 and Z_2 the atomic numbers of the projectile and the target atom, respectively, A_1 and E the atomic mass and the energy of the projectile, respectively. The equilibrium mean charge

states of ions in carbon foils have been estimated to follow semi-empirical or empirical formulas by Nikolaev and Dmitriev (ND) [24], To and Drouin (TD) [25], and Shima et al. [26]. For the present collision system, they give a value of 12.7 (ND and TD) or 12.8 (Shima et al.). Recently, Schiwietz and Grande proposed a pair of "improved" fit formulas for mean equilibrium charge states for gaseous and solid targets [27], which yields a better value of 12.6 for the present experiment.

Another characteristic feature in Fig. 2(b) is that the distribution width for S^{6+} incidence overshoots at the target thickness around $1.0\,\mu g/cm^2$, as was observed in the high energy cases of 28.9 MeV/u Pb^{56+} and 24.1 MeV/u U^{58+} ions passing through C-foils [7]. For S^{10+} incidence, a weak bump is also found at $0.9\,\mu g/cm^2$, while the distribution widths for S^{11+} and S^{13+} incidence monotonously increase as the target thickness grows.

We performed a calculation of charge state populations using the ETACHA [13,14] code, although the present projectile energy is lower than the assumed energy range of the code (over 10 MeV/u), because it is so handy for experimentalists considering that it can treat up to 28 projectile electrons in the 1s, 2s, 2p, 3s, 3p and 3d subshells. This code solves the rate equations taking accounts of the electron capture to the ground and excited states, electron loss of the ground and excited states, excitation and de-excitation between the ground and an excited state or between excited states, and radiative and Auger decays. Also the energy loss of projectile can be considered to modify the cross sections for thick targets, but this has not been employed here. The results are plotted in Figs. 1, 2(a) and 2(b) for the charge state distributions, the mean charge states and the widths derived from the calculated distributions, respectively. The general feature of the evolution of the mean charge state and the distribution width with the target thickness seems to be reproduced fairly well by the code as illustrated in Fig. 2, except for following two discrepancies. The first is that the near equilibrium mean charge state derived by the code falls on 13.0, which is larger than the experimental value by 5%. Taking a look in Fig. 1, this shift is found to come from the fact that the calculated fractions for higher charge states

over 13+ exceed the experimental fractions at 6.9 μg/cm^2 for S^{6+} incident case and at 4.7 μg/cm^2 for S^{10+}, S^{11+} and S^{13+} incident cases, which agree with Fig. 2(a) and indicates that the ETA-CHA code comparatively overestimates the electron loss cross section than electron capture cross section for K-shell electrons. The second is that the simulated variations of the mean charge and distribution width takes places roughly twice slower than the experiment, which suggests that the actual cross sections of the electron capture and loss processes are roughly a factor of 2 larger than those adopted in the simulation. It can be seen in Fig. 1 that the lower charge state distributions below 11+ for the thinner targets (0.9–1.5 μg/cm^2) agree with the calculated results for 2.0–3.0 μg/cm^2 for the S^{6+} and S^{10+} incident cases, indicating that the ETACHA code keeps a good balance in the cross sections for L-shell processes of electron capture and loss although the cross sections are estimated as low as half of the experiment.

It can be said that for the ion–solid collisions of clothed projectiles at a few MeV/u, (1) the scenario of the ETACHA code which includes the 1s to 3d subshells as electronic states and traces the processes of electron capture, loss, excitation, de-excitation and radiative and Auger decays satisfactorily explains the experiment, and (2) better agreement can be achieved if (2a) values of the collisional cross sections of electronic transitions for L-shell processes are replaced with larger ones (roughly by a factor of 2), and (2b) relatively larger values for the electron capture cross sections are employed compared with the electron loss cross sections for K-shell processes.

References

[1] N. Bohr, J. Lindhard, K. Dan, Vidensk. Selsk. Mat. Fys. Medd. 28 (1954) 7.

[2] U. Majewska, J. Braziewicz, M. Polasik, K. Słabkowska, I. Fijał, M. Jaskóła, A. Korman, S. Chojnacki, W. Kretschmer, Nucl. Instr. and Meth. B 205 (2003) 799.

[3] P. Sigmund, Phys. Rev. A 50 (1994) 3197.

[4] A.B. Wittkower, H.D. Betz, At. Data Nucl. Data Tables 5 (1973) 5.

[5] K. Shima, T. Mikumo, H. Tawara, At. Data Nucl. Data Tables 34 (1986) 357.

[6] K. Shima, N. Kuno, M. Yamanouchi, H. Tawara, At. Data Nucl. Data Tables 51 (1992) 173.

[7] A. Leon, S. Melki, D. Lisfi, J.P. Grandin, P. Jardin, M.G. Suraud, A. Cassimi, At. Data Nucl. Data Tables 69 (1998) 217.

[8] H.D. Betz, L. Grodzins, Phys. Rev. Lett. 25 (1970) 211.

[9] K. Shima, S. Ishii, T. Takahashi, I. Sugai, Nucl. Instr. and Meth. A 460 (2001) 233.

[10] H.D. Betz, Rev. Mod. Phys. 44 (1972) 465.

[11] T.J. Gray, C.L. Cocke, R.K. Gardner, Phys. Rev. A 16 (1977) 1907.

[12] C. Scheidenberger, Th. Stöhlker, W.E. Meyerhof, H. Geissel, P.H. Mokler, B. Blank, Nucl. Instr. and Meth. B 142 (1998) 441.

[13] J.P. Rozet, A. Chetioui, P. Piquemal, D. Vernhet, K. Wohrer, C. Stéphan, L. Tassan-Got, J. Phys. B 22 (1989) 33.

[14] J.P. Rozet, C. Stéphan, D. Vernhet, Nucl. Instr. and Meth. B 107 (1996) 67.

[15] R.B. Clark, I.S. Grant, R. King, D.A. Eastham, T. Joy, Nucl. Instr. and Meth. 133 (1976) 17.

[16] U. Scharfer, C. Henrichs, J.D. Fox, P. von Brentano, L. Degener, J.C. Sens, A. Pape, Nucl. Instr. and Meth. 146 (1977) 573.

[17] K. Shima, E. Nakagawa, T. Kakita, M. Yamanouchi, Y. Awaya, T. Kambara, T. Mizogawa, Y. Kanai, Nucl. Instr. and Meth. B 33 (1988) 212.

[18] H.D. Betz, R. Höppler, R. Schramm, W. Oswald, Nucl. Instr. and Meth. B 33 (1988) 185.

[19] M. Sataka, M. Imai, K. Kawatsura, K. Komaki, H. Tawara, A. Vasilyev, U.I. Safronova, Phys. Rev. A 65 (2002) 052704.

[20] M. Imai, M. Sataka, S. Kitazawa, K. Komaki, K. Kawatsura, H. Shibata, H. Tawara, T. Azuma, Y. Kanai, Y. Yamazaki, Nucl. Instr. and Meth. B 193 (2002) 674.

[21] M. Imai, M. Sataka, H. Naramoto, Y. Yamazaki, K. Komaki, K. Kawatsura, Y. Kanai, Nucl. Instr. and Meth. B 67 (1992) 142.

[22] Y. Sugiyama, Y. Tomita, H. Ikezoe, E. Takekoshi, K. Ideno, N. Shikazono, Nucl. Instr. and Meth. A 281 (1989) 512.

[23] F. Besenbacher, J.U. Andersen, E. Bonderup, Nucl. Instr. and Meth. 168 (1980) 1.

[24] V.S. Nikolaev, I.S. Dmitriev, Phys. Lett. A 28 (1968) 277.

[25] K.X. To, R. Drouin, Phys. Scr. 14 (1976) 277.

[26] K. Shima, T. Ishihara, T. Mikumo, Nucl. Instr. and Meth. 200 (1982) 605.

[27] G. Schiwietz, P.L. Grande, Nucl. Instr. and Meth. B 175–177 (2001) 125.